



Geomagnetic Energy Distribution and Influence on the Ionosphere/Thermosphere in the Polar Region

Yue Deng
UNIVERSITY OF TEXAS AT ARLINGTON

02/13/2019
Final Report

DISTRIBUTION A: Distribution approved for public release.

Air Force Research Laboratory
AF Office Of Scientific Research (AFOSR)/ RTB1
Arlington, Virginia 22203
Air Force Materiel Command

DISTRIBUTION A: Distribution approved for public release.

REPORT DOCUMENTATION PAGE		<i>Form Approved</i> OMB No. 0704-0188
<p>The public reporting burden for this collection of information is estimated to average 1 hour per response, including the time for reviewing instructions, searching existing data sources, gathering and maintaining the data needed, and completing and reviewing the collection of information. Send comments regarding this burden estimate or any other aspect of this collection of information, including suggestions for reducing the burden, to Department of Defense, Executive Services, Directorate (0704-0188). Respondents should be aware that notwithstanding any other provision of law, no person shall be subject to any penalty for failing to comply with a collection of information if it does not display a currently valid OMB control number.</p> <p>PLEASE DO NOT RETURN YOUR FORM TO THE ABOVE ORGANIZATION.</p>		
1. REPORT DATE (DD-MM-YYYY) 28-02-2019	2. REPORT TYPE Final Performance	3. DATES COVERED (From - To) 15 Nov 2015 to 14 Nov 2018
4. TITLE AND SUBTITLE Geomagnetic Energy Distribution and Influence on the Ionosphere/Thermosphere in the Polar Region	5a. CONTRACT NUMBER	
	5b. GRANT NUMBER FA9550-16-1-0059	
	5c. PROGRAM ELEMENT NUMBER 61102F	
6. AUTHOR(S) Yue Deng	5d. PROJECT NUMBER	
	5e. TASK NUMBER	
	5f. WORK UNIT NUMBER	
7. PERFORMING ORGANIZATION NAME(S) AND ADDRESS(ES) UNIVERSITY OF TEXAS AT ARLINGTON 1 UNIVERSITY OF TEXAS AT ARL ARLINGTON, TX 76019-0001 US		8. PERFORMING ORGANIZATION REPORT NUMBER
9. SPONSORING/MONITORING AGENCY NAME(S) AND ADDRESS(ES) AF Office of Scientific Research 875 N. Randolph St. Room 3112 Arlington, VA 22203		10. SPONSOR/MONITOR'S ACRONYM(S) AFRL/AFOSR RTB1
		11. SPONSOR/MONITOR'S REPORT NUMBER(S) AFRL-AFOSR-VA-TR-2019-0036
12. DISTRIBUTION/AVAILABILITY STATEMENT A DISTRIBUTION UNLIMITED: PB Public Release		
13. SUPPLEMENTARY NOTES		
<p>14. ABSTRACT</p> <p>The objective of the project is to improve the specification of the magnetospheric energy inputs, including both Poynting flux and particle precipitation, in the polar upper atmosphere and to determine how the ionosphere and thermosphere respond to the geomagnetic energy distribution in order to improve the predictability of this response and effects on satellite drag and high frequency (HF) wave propagation paths. We made great progresses in the following directions:</p> <ol style="list-style-type: none"> 1. Based on the Constellation Observing System for Meteorology, Ionosphere, and Climate (COSMIC) satellites observations of electron density profiles from 2009-2014, Pedersen conductivity has been estimated. A climatologic study of the heightintegrated Pedersen conductances in both E (100150 km) and F (150600 km) regions and their ratio in different seasons, solar and geomagnetic conditions has been conducted. 2. To understand the significance of different physical mechanisms including Poynting flux and particle precipitation, and the correlation between them, a statistical study of Poynting flux and particle energy flux in the dayside cusp and low-latitude boundary layer (LLBL) regions has been conducted based on DMSP F15 measurements. 3. The electric field and the particle precipitation at different spatial scale sizes have been investigated by utilizing the Dynamic Explorer 2 satellite data set, focusing on conditions of moderately strong southward interplanetary magnetic field. 4. The influence of an idealized, smaller Carrington-type storm on the thermosphere in the high latitudes has been simulated using the nonhydrostatic Global Ionosphere-Thermosphere Model. 5. The energetic electrons and ions (0.130.2 keV) measured by DMSP are binned according to geomagnetic coordinates. The polar distributions of particle precipitation are then incorporated into the Global Ionosphere-Thermosphere Model (GITM) 		
<p>15. SUBJECT TERMS Ionosphere, Polar Cap, Poynting Flux</p>		

16. SECURITY CLASSIFICATION OF:			17. LIMITATION OF ABSTRACT UU	18. NUMBER OF PAGES	19a. NAME OF RESPONSIBLE PERSON MOSES, JULIE
a. REPORT Unclassified	b. ABSTRACT Unclassified	c. THIS PAGE Unclassified			19b. TELEPHONE NUMBER <i>(Include area code)</i> 703-696-9586

Final Report

Geomagnetic Energy Distribution and Influence on the Ionosphere/Thermosphere in the Polar Region

PI: Yue Deng

Collaborators: Delores Knipp & Yanshi Huang

Contract/Grant #: FA9550-16-1-0059

Period of Performance: November, 2015 to November, 2018

1. Project Objectives

The objective of the project is to improve the specification of the magnetospheric energy inputs, including both Poynting flux and particle precipitation, in the polar upper atmosphere and to determine how the ionosphere and thermosphere respond to the geomagnetic energy distribution in order to improve the predictability of this response and effects on satellite drag and high frequency (HF) wave propagation paths.

2. Work Carried Out and Results Obtained

2.1. Dependence of Pedersen conductance on the solar and geomagnetic activities:

Ionospheric conductance is very important to the magnetosphere-ionosphere coupling especially in the high latitude region, since it correlates the polar cap potential with the currents. Meanwhile, the altitudinal distribution of Pedersen conductivity gives us a rough idea about the altitudinal distribution of Joule heating at high latitudes, which is significant to the response of the ionosphere/thermosphere to the geomagnetic energy inputs. Based on the Constellation Observing System for Meteorology, Ionosphere, and Climate (COSMIC) satellites observations of electron density profiles from 2009-2014, Pedersen conductivity has been estimated. A climatologic study of the height-integrated Pedersen conductances in both E (100–150 km) and F (150–600 km) regions and their ratio in different seasons, solar and geomagnetic conditions has been conducted. Figure 1 shows a strong dependence of conductance on F10.7 and Ap indices. Meanwhile, A significant interhemispheric asymmetry is identified in the dependence on F10.7 and AP, which also shows the variation with local time. This result will strongly help our understanding of the variation of the altitudinal energy distribution under different solar and geomagnetic conditions and the inter-hemispheric asymmetry of the high-latitude electrodynamic. The results have been reported in:

*Sheng, C., **Y. Deng**, Y. Lu, X. Yue (2017), Dependence of Pedersen conductance in the E and F regions and their ratio on the solar and geomagnetic activities, *Space Weather*, doi:10.1002/2016SW001486.

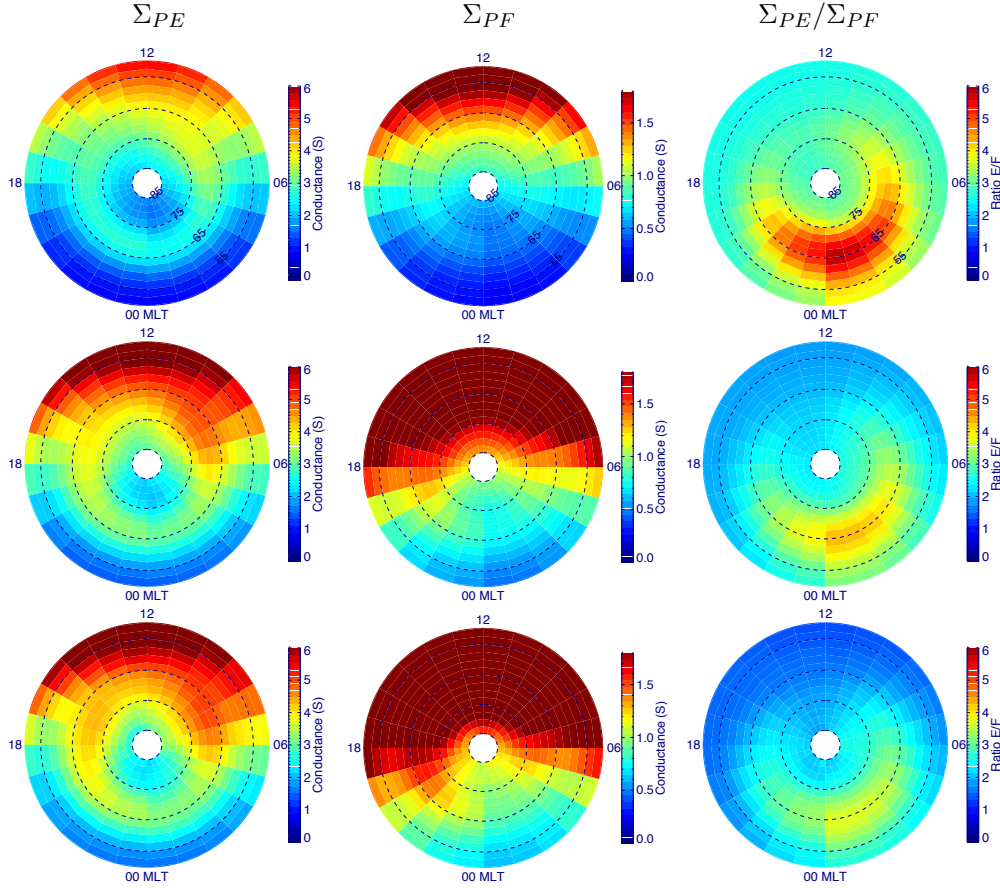


Figure 1: Σ_{PE} (left column), Σ_{PF} (middle column), and their ratio (Σ_{PE}/Σ_{PF} , right column) under different levels of solar radiation, $F10.7 < 100$ (top row), $100 < F10.7 < 150$ (middle row), and $F10.7 > 150$ (bottom row) in the northern hemisphere.

2.2. Poynting Flux in the Dayside Polar Cap Boundary Regions:

Poynting flux, which describes electromagnetic energy flux, is an important energy source for the high-latitude upper atmosphere. After the launch of Defense Meteorological Satellite Program (DMSP) F15 spacecraft with a boom-mounted magnetometer on board, there was a new opportunity to calculate Earth-directed Poynting flux at satellite altitudes (~ 850 km) in the upper atmosphere. A persistent enhancement of thermospheric density in the dayside polar cap boundary regions has been reported in the CHAMP satellite observations. To understand the significance of different physical mechanisms including Poynting flux and particle precipitation, and the correlation between them, a statistical study of Poynting flux and particle energy flux in the dayside cusp and low-latitude boundary layer (LLBL) regions has been conducted based on DMSP F15 measurements. DMSP satellite observations showed a dominate downward Poynting flux for most cases in the cusp region. Our analysis of DMSP F15 data for five years (2000–2004) reveals that approximately 53% of 660 cusp crossings at 800–850 km showed strong downward Poynting flux ($S > 10$ mW/m²), 32% of the crossings had

noticeable downward Poynting flux ($S > 3$ mW/m²), and 7% of the crossings did not show clear Poynting flux ($S < 1$ mW/m²), as shown in Figure 2. Only 13 out of 660 cusp crossings (~2%) showed noticeable upward Poynting flux. In the LLBL region, 35% of 11,641 LLBL crossings showed significant downward Poynting flux, 34% of the crossings had noticeable downward Poynting flux, and only 13% of the crossings did not show clear Poynting flux. On average, Poynting flux in LLBL is smaller than that in the cusp. The results show a slightly negative correlation between Poynting flux and particle precipitation energy flux in the dayside polar cap boundary regions. Statistically, Poynting flux in the cusp is enhanced during interplanetary magnetic field By positive conditions. The results have been reported in:

*Lu Y., Y. Deng, C. Sheng, L. Kilcommons, D. Knipp (2018), Poynting Flux in the Dayside Polar Cap Boundary Regions from DMSP F15 satellite measurements, *J. Geophys. Res.*, 123. <https://doi.org/10.1002/2018JA025309>.

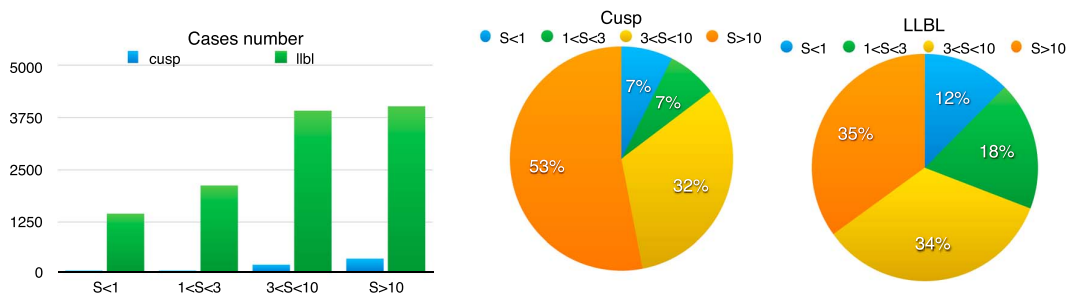


Figure 2: The histogram shows the number comparison between the cusp and LLBL in each category. The pie charts show the percentage of downward Poynting flux observations in each category. The left side is the cusp, and the right side is the LLBL.

2.3. Small-scale variability in electric field and particle precipitation:

In this study, the electric field and the particle precipitation at different spatial scale sizes have been investigated by utilizing the Dynamic Explorer 2 satellite data set, focusing on conditions of moderately strong southward interplanetary magnetic field. Dynamic Explorer 2 data from the period between 1981 and 1983, from all universal times, seasons, and both hemispheres, have been processed and binned over geomagnetic latitude and local time. It is found that, as compared with the large-scale (>500 km) average electric field and particle precipitation, the variabilities (i.e., departures from the large-scale average) of electric field and particle precipitation are not negligible. Moreover, the electric field variability tends to be anti-correlated with the particle precipitation variability in the auroral regions on small scale and meso-scale (<500 km), as shown in Figure 3. The impacts associated with the small-scale and meso-scale electric field and particle precipitation variabilities on Joule heating have also been addressed in this study by using the Global Ionosphere and Thermosphere Model. It is found that although Joule heating can be significantly enhanced by the small-scale and meso-scale electric field variabilities (~27% globally), the corresponding change in the particle precipitation tends to depress such enhancement (5% globally), which is not negligible

on the dusk side (up to 17.5% locally). It is the first time that the correlation between electric field and particle precipitation variabilities on small scale and meso-scale has been quantified. Furthermore, the impact on Joule heating associated with the correlation between the small-scale and meso-scale electric field and particle precipitation variabilities has been evaluated unprecedentedly in a general circulation model. The results have been reported in:

*Zhu, Q., **Y. Deng**, A. Richmond, A. Maute (2018), Small-scale variability in electric field and particle precipitation and its impact on Joule heating, *J. Geophys. Res.*, 123.

<https://doi.org/10.1002/2018JA025771>

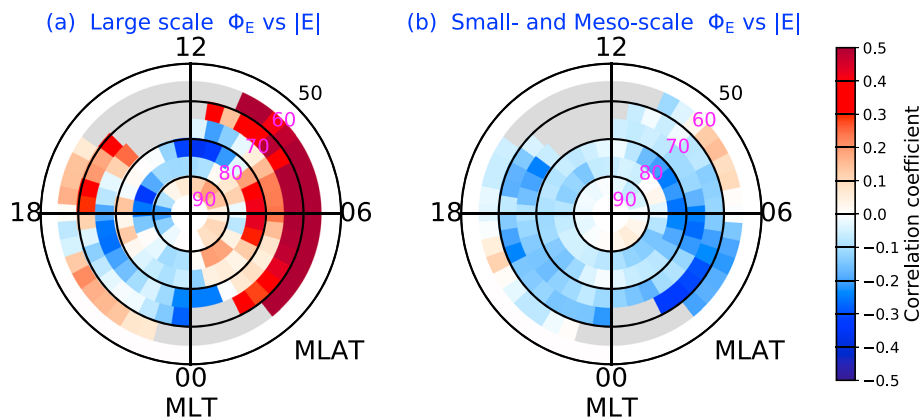


Figure 3: The distributions of the linear correlation coefficient (a) between the large-scale electric field intensity and particle energy flux and (b) between small-scale and mesoscale variabilities of electric field intensity and particle energy flux when IMF clock angle is between 135° and 225° , and IMF B_t ranges from 4 to 10 nT.

2.4. Possible influence of extreme magnetic storms:

Solar and interplanetary events can create extreme magnetic storms, such as the Carrington storm in 1859 with intensity up to $Dst \sim -1,760$ nT. The influence of an idealized, smaller Carrington-type storm on the thermosphere has been simulated using the nonhydrostatic Global Ionosphere-Thermosphere Model. For the storm conditions we simulated, the solar wind BZ and velocity were -50 nT and 1,000 m/s, respectively. The corresponding cross polar cap potential reached 360 kV, and the hemispheric power was 200 GW. Consequently, the hemispheric integrated Joule heating exceeded 3,500 GW, which is more than 70 times higher than normal conditions. The thermosphere variations at high latitudes were examined through the comparison of three cases: reference, storm with geomagnetic energy enhancement only, and storm with both solar and geomagnetic energy enhancement. At 400-km altitude, the neutral density increased by >20 times at certain locations and by >10 times globally averaged. The atmosphere experienced a temperature of 4000 K, more than 1,500 m/s horizontal wind, and exceeding 150 m/s

vertical wind. In general, additional energy increase from solar irradiation resulted in 20–30% more perturbation in neutral density and temperature. The exobase (top boundary of the thermosphere) expanded to altitudes >1,000 km, and the buoyancy acceleration (difference between vertical pressure gradient force and gravity force) can be as large as 3 m/s². The results will help to determine possible extreme responses to interplanetary coronal mass ejections for various phenomena occurring in geospace. The results have been reported in:

Deng Y., C. Sheng, B. Tsurutani, A. Mannucci (2018), Possible influence of extreme magnetic storms on the thermosphere in the high latitudes, *Space Weather*, 16.
<https://doi.org/10.1029/2018SW001847>.

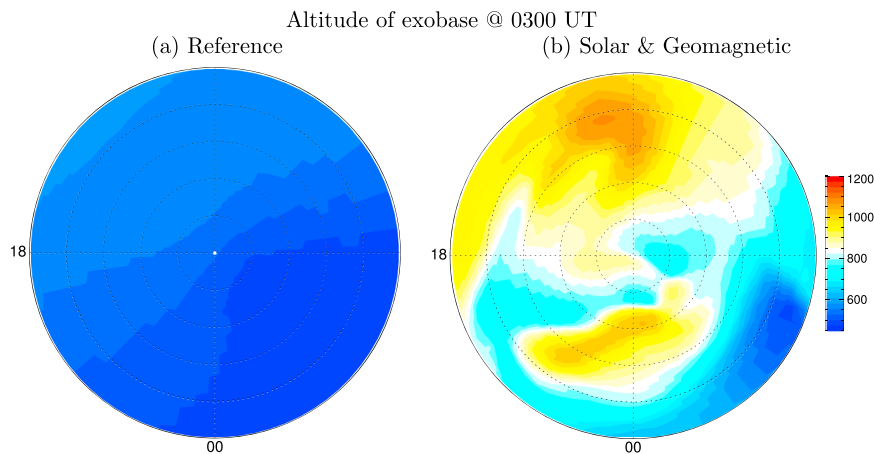


Figure 4: Altitude of exobase for the (a) reference case and (b) storm case with enhancement of both solar and geomagnetic energy at 0300 UT. The maximum altitude is close to 600 and 1,200 km for the reference and storm cases, respectively.

2.5. Effects of Particle Precipitation on Nitric Oxide Cooling:

Satellite measurements have revealed significant enhancement of nitric oxide (NO) emission at 5.3- μm during shock-led interplanetary coronal mass ejection events. The abnormal enhancement of NO cooling during shock-lead storm may contribute to the problem storms. While it is well-known the particle precipitation is primary mechanism for the NO emission enhancement, it is uncertain what is the relative significance of ions, soft electrons and kev electrons. The goal of this study is to identify contribution of ion and electron (from each energy band) particle precipitation to the thermospheric NO cooling enhancement. The energetic electrons and ions (0.1–30.2 keV) measured by DMSP are binned according to geomagnetic coordinates. The polar distributions of particle precipitation are then incorporated into the Global Ionosphere-Thermosphere Model (GITM). The results show that the electrons play dominant role to NO cooling, but the ions are important as well and can contribute up to 30% of NO cooling during geo-effective events. Among four electron bands, NO cooling enhancement during the events is dominated by the electrons in the energy band of 1.4–6.5 keV. The global

thermospheric and ionospheric responses show that both total electron content and NO cooling enhance instantaneously at the source regions, but they have different lifetime and correlation with the particle precipitations. The results have been reported in:

*Lin, C., **Y. Deng**, Delores J. Knipp, Liam M. Kilcommons (2018), Effects of Energetic Particle Precipitation on Thermospheric Nitric Oxide Cooling, *J. Geophys. Res.*, to be submitted.

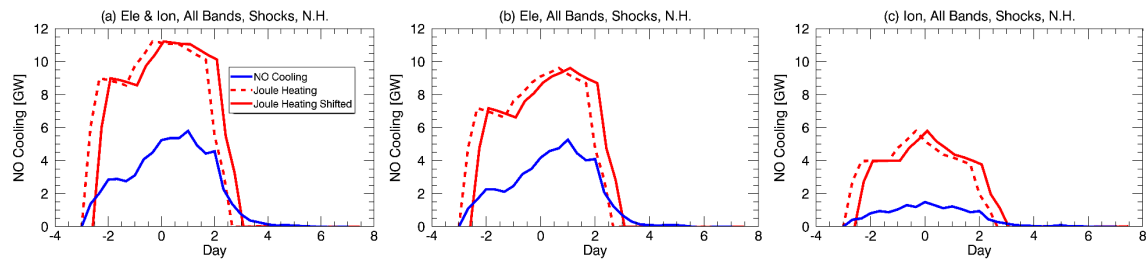


Figure 5: Enhancement of total NO cooling power poleward of 40°N (top row) during the shock-led events with (a) both electron and ion effects, (b) electron in all bands and (c) ion only.

3. Publications

1. *Sheng, C., **Y. Deng**, Y. Lu, X. Yue (2017), Dependence of Pedersen conductance in the E and F regions and their ratio on the solar and geomagnetic activities, *Space Weather*, doi:10.1002/2016SW001486.
2. *Lu Y., **Y. Deng**, C. Sheng, L. Kilcommons, D. Knipp (2018), Poynting Flux in the Dayside Polar Cap Boundary Regions from DMSP F15 satellite measurements, *J. Geophys. Res.*, 123. <https://doi.org/10.1002/2018JA025309>.
3. *Zhu, Q., **Y. Deng**, A. Richmond, A. Maute (2018), Small-scale variability in electric field and particle precipitation and its impact on Joule heating, *J. Geophys. Res.*, 123. <https://doi.org/10.1002/2018JA025771>.
4. **Deng Y.**, C. Sheng, B. Tsurutani, A. Mannucci (2018), Possible influence of extreme magnetic storms on the thermosphere in the high latitudes, *Space Weather*, 16. <https://doi.org/10.1029/2018SW001847>.
5. *Lin, C., **Y. Deng**, Delores J. Knipp, Liam M. Kilcommons (2018), Effects of Energetic Particle Precipitation on Thermospheric Nitric Oxide Cooling, *J. Geophys. Res.*, to be submitted.

***: Advised graduate student and postdoc publications.**